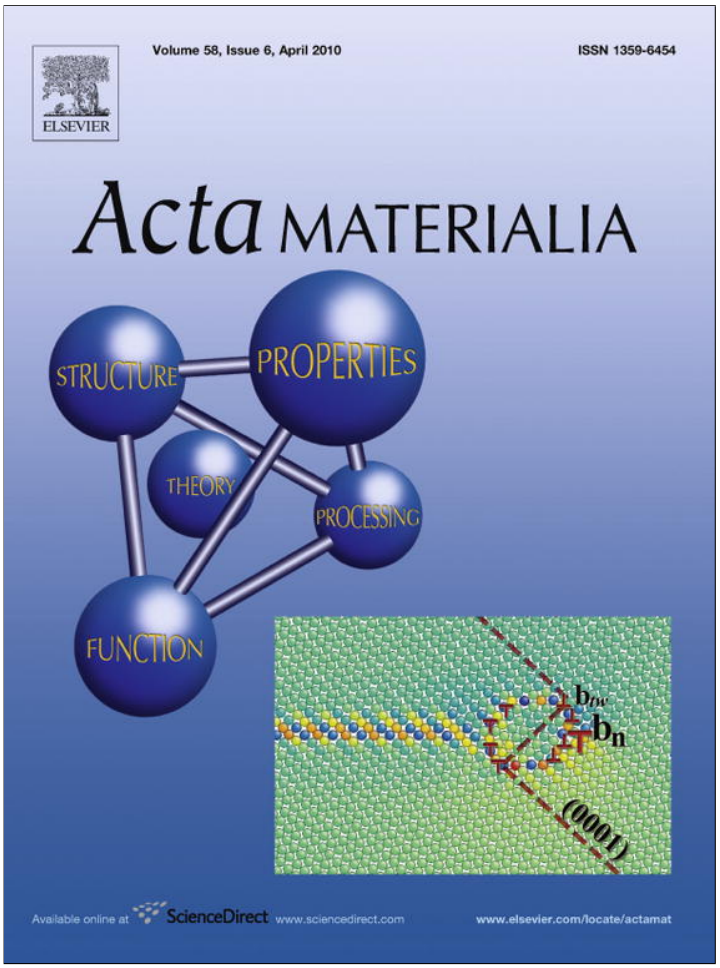

Available online at www.sciencedirect.com
ScienceDirect
Acta Materialia 58 (2010) 2068–2078
Acta MATERIALIA
www.elsevier.com/locate/actamat

Role of substrate commensurability on non-reactive wetting kinetics of liquid metals

M. Benhassine [a], E. Saiz [b,1], A.P. Tomsia [b], J. De Coninck [a,*]

[a] Centre for Research in Molecular Modelling, University of Mons-Hainaut, Parc Initialis, Av. Copernic, 1, 7000 Mons, Belgium
[b] Materials Sciences Division, Lawrence Berkeley National Laboratory, Berkeley, CA 94720, USA

Received 22 September 2009; received in revised form 25 November 2009; accepted 26 November 2009
Available online 6 January 2010

Abstract

The dynamics of spreading of liquid metal atoms via molecular dynamics is considered vs. the commensurability of the solid surface with respect to the size of the liquid atoms. The solid surfaces are modeled as rigid (1 0 0) oriented Ni and, for two series of simulations, the lattice spacing of the substrate is varied from the regular equilibrium spacing to a commensurate situation with Au or Ag drops spreading spontaneously on top. The diffusion is calculated in the layered region of the liquid in contact with the two different solid surfaces and then compared. Then, the dynamic evolution of the contact angle is fitted to Molecular Kinetic Theory and compared with the two substrate geometries. It is observed that the friction parameter scales as the inverse of the diffusion in the interfacial region. The change in ordering induced by the commensurate substrate is characterized by examining the density profiles across the solid/liquid interface and fitting the curve by an exponential decay with a characteristic correlation distance $1/\kappa$. It is shown that the commensurability/non-commensurability of the solid surface with respect to the liquid atoms changes the ordering, which plays a significant role in the dynamics, a feature not properly taken into account in the present formulation of Molecular Kinetic Theory.

Keywords: High-temperature spreading; Diffusion; Wetting; Liquid metals; Molecular dynamics

1. Introduction

Wetting in metallic systems is of great importance in many industries, such as microelectronics, aerospace and automobile to name just a few. In many applications, it is necessary to control the dynamics of the processes considered. The dynamics of wetting for non-reactive liquid metals has been a subject of intense research over the last few years [1–5]. For these low viscosity and high surface tension liquids, it has been shown that the mechanism controlling the dynamics of wetting is the friction dissipation at the three-phase line where the substrate, liquid metal and air/vacuum meet [1–3]. This channel of dissipation is described by Molecular Kinetic Theory (MKT), due to T.D. Blake, as demonstrated in several experiments and simulations [7–11] (and references therein).

The MKT of wetting describes the dynamics of wetting at the atomic level by a reaction-rate model controlled by a certain jump frequency of liquid atoms at equilibrium K_0 and a characteristic length λ. The end result is the movement of the triple line as a result of collective behavior dictated by the equilibrium parameters (K_0, λ) [7].

The critical frequency of the rate-determining step K_0 can be evaluated by a fitting procedure or can be calculated if one has access to the atomic trajectories vs. time, as in molecular dynamics. This interesting computational tool, if the model is trustworthy, can give deep insight into the atomic events occurring at the liquid/solid interface, a region which is difficult to approximate by continuum models.

* Corresponding author.
E-mail address: joel.deconinck@umons.ac.be (J. De Coninck).
[1] Present address: UK Center for Structural Ceramics, Department of Materials, Imperial College, London, UK.

1359-6454/$36.00 © 2009 Acta Materialia Inc. Published by Elsevier Ltd. All rights reserved.
doi:10.1016/j.actamat.2009.11.049

Another interesting and well-studied variable for characterizing such liquid metals is the diffusion parameter at the vicinity of the solid surface. It was pointed out by Deltour [6] that, in the case of a commensurate substrate, the diffusion coefficient in an atomic cluster of atoms near the substrate (D_s) tends to zero with the existence of an energy barrier to overcome in order to make the cluster advance. Changing the commensurability thus modifies the diffusion coefficient near the interface D_s, within a Lennard–Jones fluid. The link between this jump frequency K_0 and the diffusion constant is not obvious, but it seems reasonable to expect that if K_0 is high the mobility of atoms is enhanced, and D_s has to be large and vice versa.

This is precisely the object of the present paper: to investigate how the geometry of the substrate affects the values of K_0 and λ as well as the diffusion constants, and whether the results of a small cluster at room temperature studied by Deltour are still applicable with a metallic liquid drop in a high-temperature environment.

By means of molecular dynamics simulations for two liquid metals, Ag and Au, this link was analyzed by studying the diffusivity of the liquid atoms and the spreading dynamics of sessile drops vs. the spacing between the solid atoms for a rigid surface made of Ni atoms to account for an inert, strictly non-reactive wetting system. This simulation methodology and choice has been discussed in prior simulations [3].

The paper is organized as follows: Section 2 describes the model and introduces the pertinent variables; Section 3 is devoted to the results of the simulations and their discussion. The concluding remarks are presented in Section 4.

2. The model

To perform molecular dynamics simulations of wetting, the parallel code LAMMPS [14,15] was used. The simulations consisted in modeling drops of pure Ag and pure Au liquids (36982 atoms) with an embedded atom method potential [16,17].

In the first simulation, the drops were equilibrated for 50 ps and then shifted before spreading just above the upper (1 0 0) surface of a fixed face-centred cubic (fcc) Ni solid with a lattice parameter of 3.52 Å (called a regular substrate or RS). The Ni atoms were purposely fixed to model an ideally non-reactive situation and to be able to vary the distance between the atoms in the surface. More precisely, if the atoms were mobile, or alternatively were tethered via some harmonic potential to their initial positions, this procedure would make it more difficult to study a commensurate effect, because the Ni atoms would relax to their equilibrium lattice distance at the considered temperature. This type of methodology was used by Benhassine et al. [3] and Hashibon et al. [18] to account for an ideal non-reactive solid surface, such as molybdenum [3] or a ceramic [18], with a very high melting temperature.

In the second simulation, the lattice spacing of the substrate was changed (fcc 4.09 Å) to reflect the Ag equilibrium configuration (in the case of Au, it was changed to fcc 4.08 Å); these solids are called commensurate substrates (CS). This allowed observation of the effect of this lattice change on the kinetics of spreading and on the diffusivity of the Ag and Au atoms in the vicinity of the solid surface with respect to the geometry of the solid. Experimentally, this study is relevant, because in the different crystalline phases of the surface, the interatomic distance can vary, and the different surfaces can become closer to a commensurate situation.

The time step was 1 fs, and configurations were saved every 0.01 ns or 0.001 ns. A constant number of particles was used, and a volume ensemble with an ad hoc rescaling of the temperature every 10 fs, accounting for the constant temperature environment of a furnace, making the comparison with the present experiments [1,2] more straightforward. Because the substrate was fixed, i.e., the forces calculated on the solid atoms were zero, the temperature rescaling only accounted for atoms in the Ag and Au drops. Although all the simulations were performed in the classical sessile-drop configuration, a liquid column configuration with periodic boundary conditions in the x, y direction, which accounts for a proper equilibrium system, was also simulated following the same methodology as that discussed in Ref. [3]. The solids considered in the present study always have the (1 0 0) plane as a free surface, as was also the case in Ref. [3], whether referring to a sessile drop or a liquid column. In the particular case of the column, the free surfaces remained the (1 0 0) surfaces, and this plane was modeled as infinite because of the periodic boundary condition.

2.1. Molecular kinetic theory

The MKT of wetting [12,13] relates the speed of the triple junction v and the dynamic contact angle θ_D to equilibrium parameters, which are the equilibrium contact angle θ_0, the frequencies K_0 of jumps of the liquid atoms, and amplitude of displacement λ. The relation is as follows:

$$v = 2K_0\lambda \sinh\left(\frac{\gamma_{lv}}{2nk_BT}(\cos\theta_0 - \cos\theta_D)\right) \tag{1}$$

where n is the density of adsorption sites on the surface, k_B is Boltzmann's constant, T is the liquid temperature, and γ_{lv} is the liquid/vapor surface tension. The three-phase line advancement is the result of a complex collective motion, and the key is to obtain the rate-determining atomic step which controls the movement of the triple junction and its related effective λ.

This equation can be linearized if the argument of the sinh becomes small (which corresponds to a situation close to equilibrium), and the unknown parameters K_0, λ and n can be coupled into one single parameter called the triple-line friction ζ_0, defined as $\zeta_0 = \frac{nk_BT}{K_0\lambda}$. Eq. (1) then becomes

$$v = \frac{\gamma_{lv}}{\zeta_0}(\cos\theta_0 - \cos\theta_D) \tag{2}$$

2.2. Diffusion in the interfacial region

To study diffusion, the quadratic displacement of the center of mass of the liquid particles in the molecular dynamics simulations vs. time is evaluated, and D is determined when t is very large, such that

$$\frac{R^2(t)}{t} \underset{t\to\infty}{\rightarrow} D \tag{3}$$

D is proportional to the diffusion coefficient, and $R^2(t)$ is calculated as

$$R^2(t) = \frac{1}{N}\sum_{i=1}^{N}[(x_i(t)-x_{i0})^2 + (y_i(t)-y_{i0})^2 + (z_i(t)-z_{i0})^2] \tag{4}$$

(x_{i0}, y_{i0}, z_{i0}) denotes the position of atom i at time 0. For calculation of the diffusion in a fixed zone of space (such as in a few layers of the liquid in contact with a solid surface), it is verified that the atoms which contribute to the calculation of $R^2(t)$ always stay in the same region during the simulation. It is important here to say that the diffusion is calculated in a slab of liquid. Therefore, the diffusion along the z-axis is not going to be in a linear regime at later times, since the atom could reach the boundaries of the slab very fast (the atoms that cross the boundary of calculation are omitted) and the condition of Eq. (3) will not hold true.

Eq. (4) is general, but this study focuses on the particular case of the diffusion in the interfacial region of the liquid, which comprises a few layers. In this case, Eq. (4) is simplified as

$$R^2_{x,y}(t) = \frac{1}{N}\sum_{i=1}^{N}\left[(x_i(t)-x_{i0})^2 + (y_i(t)-y_{i0})^2\right] \tag{5}$$

and diffusion becomes the in-plane diffusion $D_{x,y}$. Indeed, the density profiles demonstrate that the concentration is not homogeneous across the solid/liquid interface, and so the diffusion is supposed to evolve discontinuously. The calculated diffusion presented here thus accounts for an effective movement of atoms in the layered region of the liquid in contact with the solid. It is therefore intended to evaluate the correlation between the diffusion in the interfacial region and the vision of dynamic wetting depicted by MKT.

In previous work [3] it was shown that the perpendicular displacements, or frequencies defined by the molecular kinetic model, were the limiting factor in the process of wetting, and also that these jumps were linked to the density of holes or vacancies in the liquid. Thus, if the diffusion is fast, it means that there are many vacancies and that the frequencies will inevitably be higher (the lower friction being proportional to the inverse of frequency K_0).

3. Results

The equilibrium interatomic distance for Ag atoms is 4.09 Å [27]. Thus, to obtain commensurability, the lattice spacing of the solid substrate is also fixed at 4.09 Å. To visualize the difference in the two configurations, the first layer of the liquid in contact with the first (1 0 0) layer of the solid is displayed in Fig. 1. With the commensurate solid, Ag and Ni atoms coincide with each other, while this is not the case with the RS where the lack of mismatch induces less ordering in the liquid in an equilibrated state.

Snapshots from simulations with the RS and CS are given in Figs. 2 and 3, respectively.

3.1. Diffusion

First, the diffusion coefficient in Ag and Au in the area close to the interface for the two substrate configurations is calculated. The diffusion of atoms over a surface is a physical quantity which is relevant to many processes, such as evaporation or condensation.

Simulations of Ag on fixed Ni have revealed [3] that a sessile-drop configuration is a situation where equilibrium is hardly obtained in the present simulations with 30,000 liquid atoms or more, because there is still a net flow of

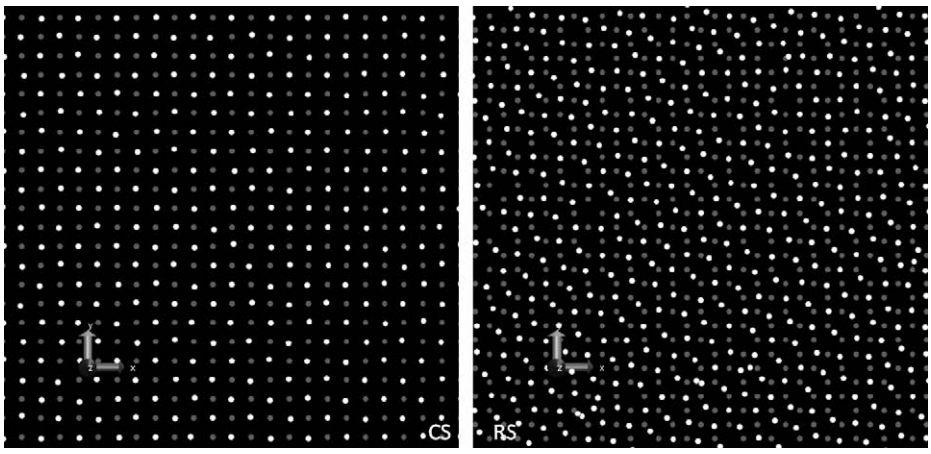

Fig. 1. Top view of the first layer of liquid Ag (in white) in contact with the (1 0 0) plane of a Ni CS (grey atoms) on the left. The regular (1 0 0) oriented Ni is displayed on the right with less ordering in the liquid Ag.

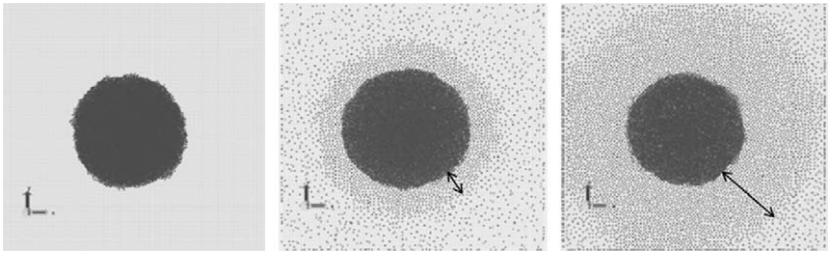

Fig. 2. Different snapshots of the spreading of an Ag drop on the regular 3.52 fcc fixed Ni substrate. The adsorbed layer is highlighted. The snapshots are taken after equilibration $t = 0$, at $t = 2$ ns and $t = 10$ ns.

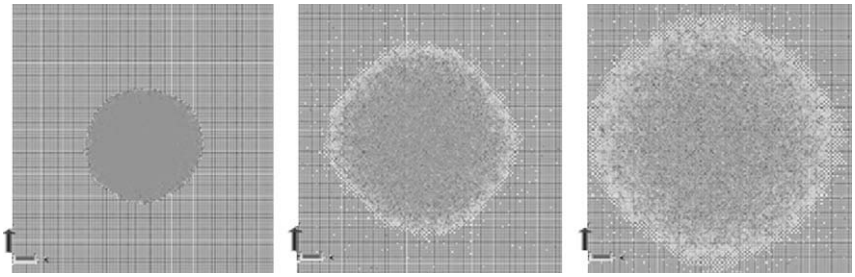

Fig. 3. Snapshots of a wetting Ag drop on the CS. The presence of an adsorbed layer is not apparent in the time frame of the run (images taken at start, 2 and 10 ns after equilibration).

atoms moving, spreading and evaporating [3] after 10 ns. Since the jump frequency is an equilibrium parameter, the calculations of $D_{x,y}$ and K_0 are made in a system which accounts for an equilibrium configuration: a column of the same liquid Ag or Au liquid with periodic boundary conditions on top of the same fixed Ni substrates. It was previously shown how the absence of free surfaces in (x, y) enables an equilibrium system to be reached faster and provides a better window of calculation (the frequency calculations are made from a point at equilibrium up to the end of the simulation) [3].

The diffusion coefficient is evaluated in the (x, y) direction from a distance from the interface between 0 and 20 Å in z, which corresponds to the layered region in the liquid according to density profiles (Fig. 4). This way reflects the rate of creation of holes in the zone where the wetting rate-controlling process is occurring [3]. The values are averaged for >2000 atoms present in the interfacial region.

The mean displacement is calculated in the plane vs. the square root of time, or $R_{x,y} = \sqrt{D_{x,y}}\sqrt{t}$ (note that $\langle R\rangle = f(\sqrt{t})$ not $\langle R^2\rangle = f(t)$ is plotted, as this yields less error, supposing that the diffusion coefficient will be stationary later). Thus the diffusion of Ag on the regular Ni substrate (Ni $\langle 1\,0\,0\rangle$ 3.52 fcc) is first calculated by evaluating the variation in the mean displacement of the center of mass of the atoms in the layered region vs. the square root of time (Fig. 5). For the CS, the slope of the curve value is 9.734 (0.960) (Å $\mathrm{ns}^{-1/2}$) or 9.475×10^{-10} $\mathrm{m^2\,s^{-1}}$. To obtain an absolute diffusion coefficient value, one needs to divide this value by 4 (or $2 \times n$, where n is the dimension). This value is much lower than the reported values [28] of simulations in bulk Ag and Au with MD simulations (of order 10^{-8} $\mathrm{m^2\,s^{-1}}$), owing to the fact that there are fewer vacancies in the ordered region than in the bulk.

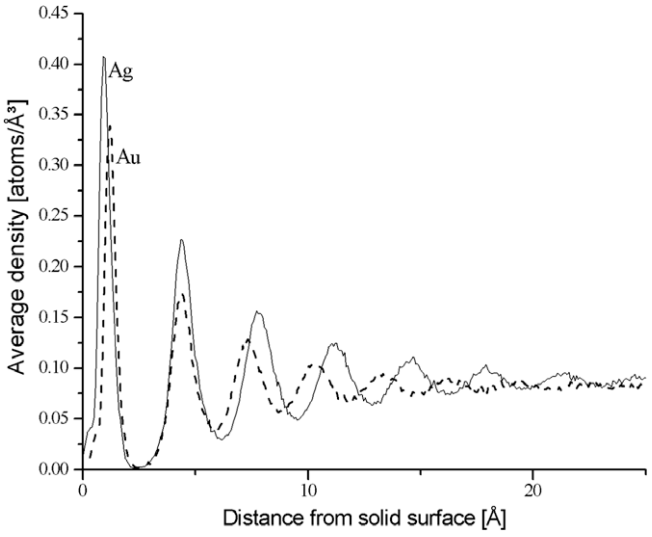

Fig. 4. Averaged density profiles showing the ordering induced by the solid surface on the liquid. At a distance ~20 Å from the interface, the density reaches that of the bulk for both Ag (solid line) and Au (dashed line).

The diffusion is also evaluated for Ag on the RS, and the slope of the curve turns out to be 96.898 (0.803) (Å $\mathrm{ns}^{-1/2}$) in this case. A strong variation in the diffusion is thus observed in the liquid close to the solid–liquid interface with a change in the distance of the atoms of the solid, which accounts for a perfect match between Au or Ag at the interface with Ni.

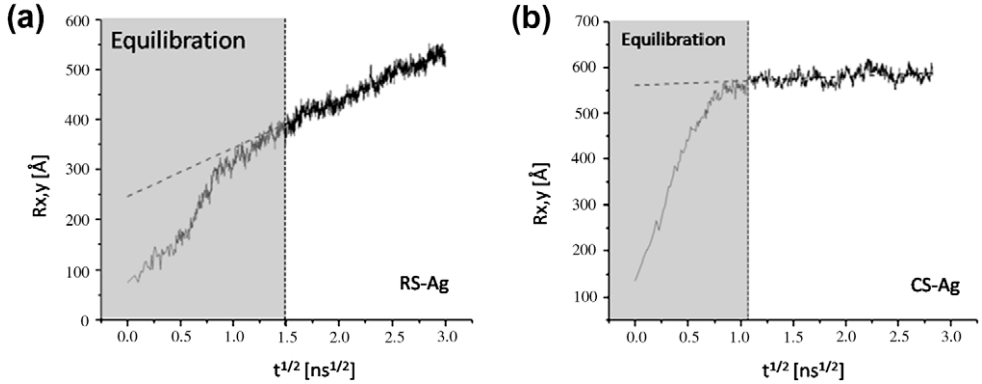

Fig. 5. Time evolution of the averaged displacements of the Ag atoms in the interfacial region on top of: (a) the RS and (b) the CS. The slope is directly proportional to the diffusion coefficient. Data from the initial equilibration times (shaded area) are not used in the calculation.

The same methodology is applied for Au (CS and RS; Fig. 6), and the results are shown in Table 1.

3.2. Dynamics of wetting

Valignat et al. [29] point out that a change in the amplitude of the interactions between polymeric liquid atoms and solid atoms can make a wetting transition from partial to complete wetting with a precursor film. In this study, changing the geometry of the substrate (by varying the spacing between solid atoms) also influences the amplitude of the interactions by modulating the surface density. In the case of the RS, the growth of a similar adsorbed layer is observed here. In the commensurate case, there is no evidence of such a layer extending away from the drop.

The growth or lack of growth of an "adsorbed layer" or monoatomic film has been observed in simple metallic systems [21,25,31]. Usually, the presence of films is associated with a complete wetting situation but, in the simulations presented here, the contact angles relax to equilibrium values which are clearly non-zero, even if one lets the drops relax for a longer time. In the partial wetting case, the drop-on-film situation has been referred to in the literature as pseudo-partial wetting (as defined by Brochard-Wyart [30]), although some authors do not make a distinction and still refer to it as partial wetting. This adsorbed layer grows on the solid surface by surface diffusion from the triple junction.

With the RS, a monoatomic film is clearly visible ahead of the triple line reflecting the adsorption of atoms coming directly from the outer surface of the drop (Fig. 2). Direct visualization of the flow in a cylindrical projection of the Ag drop on the RS demonstrates this in Fig. 7.

Surprisingly, in the commensurate situation (the substrate which has the same lattice parameter as the solid Ag (4.09 Å)), no film is observed (Fig. 3). By the construction of the solid, the spacing between silver atoms coincides with the CS. The drop consequently locks into a low-energy epitaxial configuration, because the wells of the potential generated by Ni atoms fit with Ag in the first layer in contact with the solid. The liquid thus acts like a dented wheel; whenever an atom of liquid comes in contact with the solid surface, the attraction is so great that it is trapped by one of the potential wells generated by the solid particles (via the solid–liquid interaction potential).

The two different situations (CS, RS) change the way in which the first layer is ordered: solid-like in CS, while remaining liquid though semi-ordered by the solid in RS. In the primer, any atom contributing to the wedge advancement comes from the edges, as demonstrated by

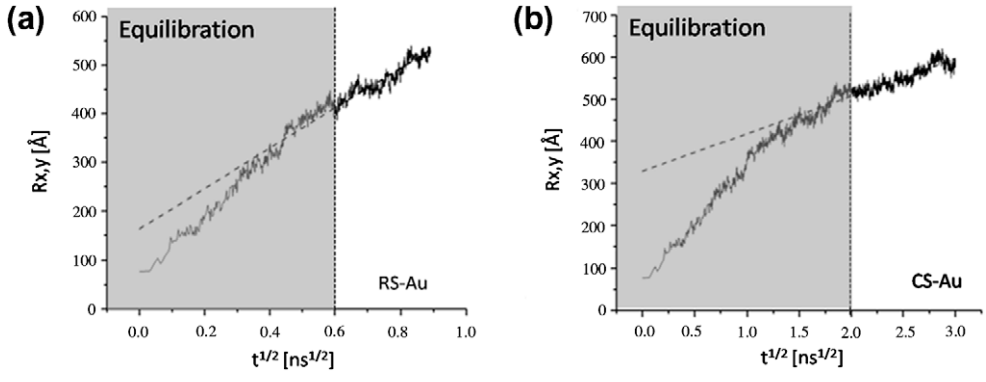

Fig. 6. In-plane displacements in the layered zone for Au on: (a) the RS and (b) the CS with the corresponding linear fits. The fit are performed after the displacements reach a linear regime.

Table 1
Value of the different diffusion constants for Au and Ag.

	$\sqrt{D_{x,y}}$ for RS (Å ns$^{-1/2}$) (error)	$\sqrt{D_{x,y}}$ for CS (Å ns$^{-1/2}$) (error)
Ag 1200 K	96.898 (0.803)	9.734 (0.960)
Au 1400 K	413.654 (3.685)	89.424 (1.018)

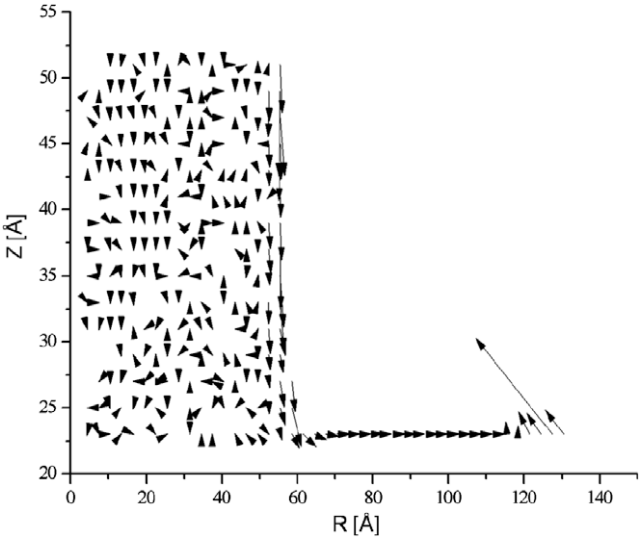

Fig. 7. Flow visualization for the Ag drop on the RS–Ni substrate in a cylindrical basis (R, z) from 8 to 10 ns. The film is "fed" by the atoms at the external surface of the liquid and do not seem to originate from the base of the drop.

the flow profiles, and the second layer spreads on a fixed layer of atoms of the same type (above the solid) as if on a perfectly smooth surface with no roughness. The radial distribution functions of the first and second layers are presented for Ag for the two situations in Fig. 8. The first-neighbor peak is absent in the second layer of the commensurate, and the first layer of the RS simulation reveals less ordering and a liquid structure.

Concerning the dynamics, in the commensurate case, equilibrium is reached more slowly than on RS (which was attained after 0.4 ns). In fact, a plateau in radius dynamics is only obtained for the very end of the simulation, and the film growth is impaired. Whenever an atom from the drop reaches the surface, it is pinned on it (in a sense, the first layer growths in epitaxy with the solid). As a consequence, surface diffusion of the liquid atoms on the solid surface is very slow, and the adsorbed film does not form during the simulation.

To measure the contact angle and radius of the spreading drop, the cylindrical (R, z) projection of the drop fit is, as usual [11,22,23], by the best-fit circular profile (which gives the base radius of the circle and its angle). The contact angle and radius dynamics are presented in Fig. 9. For clarity, only the relevant points of the dynamics are shown. For the RS, the contact angle reaches a ~90° angle in 0.4 ns, which remains constant during the remainder of the simulation (over 10 ns). The 32,000 atom-drops yield a stable contact angle, whereas smaller drops (~5000 atoms) give inconsistent results due to finite size effects (and the finiteness of the reservoir feeding the grown film). From curves $\theta(t)$ and $R(t)$, the speed $V(t)$ can be extracted by the method described by Seveno et al. [24]: a ratio of polynomials of different degrees is used to fit the radius data, and the best fit among the polynomial orders is taken. The speed is then obtained by simple derivation. This method has been experimentally validated [24]. The G-dyna freeware [24] was used to generate the different fittings of the simulations.

The data ($\theta(t)$, $V(t)$) can be fitted using the linear molecular kinetic model. With this fitting, the spacing is coupled with the frequency in the triple-line friction parameter (see Eq. (2)). The fittings are displayed in Figs. 9–12.

With the CS, the contact angle relaxes to ~11° after 30 ns. The data set can still be fitted using linear MKT, but the fitted friction is in this case 10 times lower.

For Au, the dynamics are very similar to those of Ag. The contact angle reaches a stationary value of ~90° after only 0.3 ns with the RS substrate. Consequently, the remaining part of the curve is not taken into account. The curve $R(t)$ is interpolated by a ratio of polynomials and derived as explained for Ag. In the commensurate case, the contact angle relaxes to ~60°.

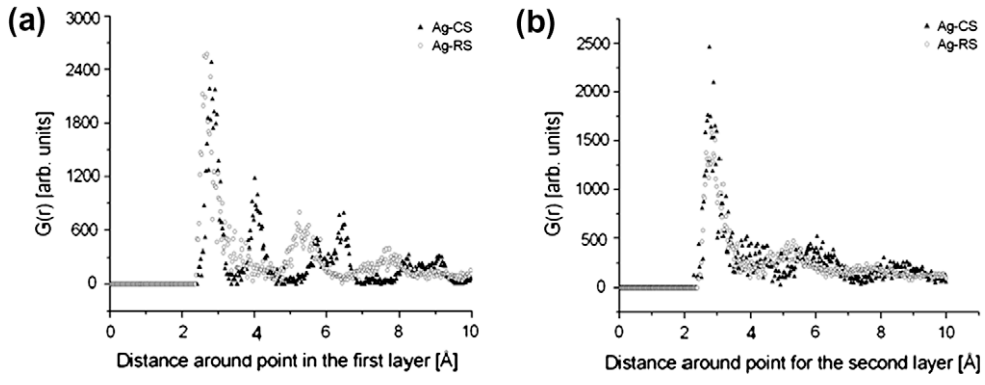

Fig. 8. Radial distribution functions $g(r)$ for the first: (a) and second (b) layers in Ag on CS and RS solids. The first layer of Ag on the CS is solid-like, as revealed by the first-neighbor peak absent in the RS substrate and in the second layers of either CS or RS.

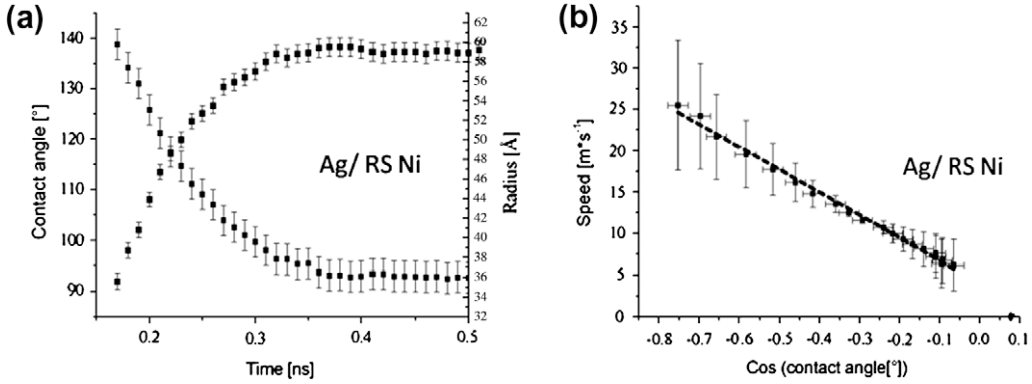

Fig. 9. (a) Base radius and contact angle vs. time for Ag on the 3.52 fcc fixed Ni solid. The error bars assume an error on the contact angle of 3°, and the radius error is determined based on this error with the spherical cap approximation. (b) The dynamics are displayed on the right side of the figure. The error bars on the speed are determined by the bootstrap method by G-dyna, and the error on the contact angle is also fixed at 3°.

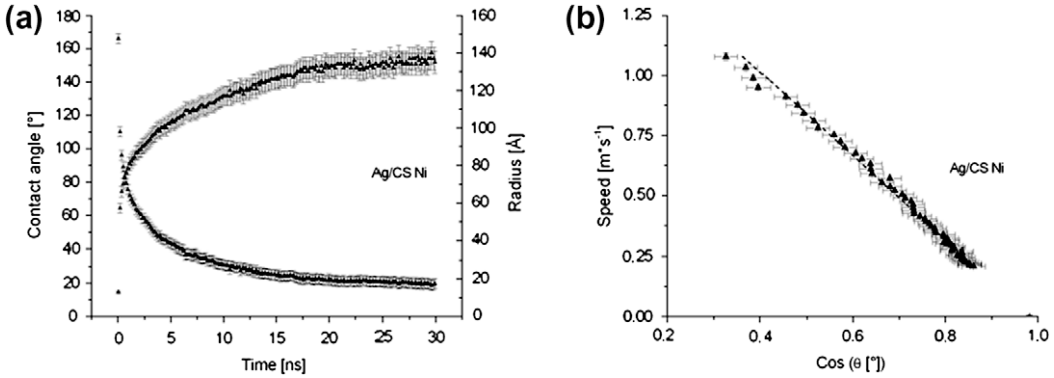

Fig. 10. (a) The contact angle and radius for Ag spreading on a 4.09 substrate (CS) is displayed on the left side of the figure. The curve $\theta(V)$ is then generated by G-dyna and fitted via a Levenberg–Marquardt procedure. (b) The equilibrium point corresponding to $v = 0$ is highlighted.

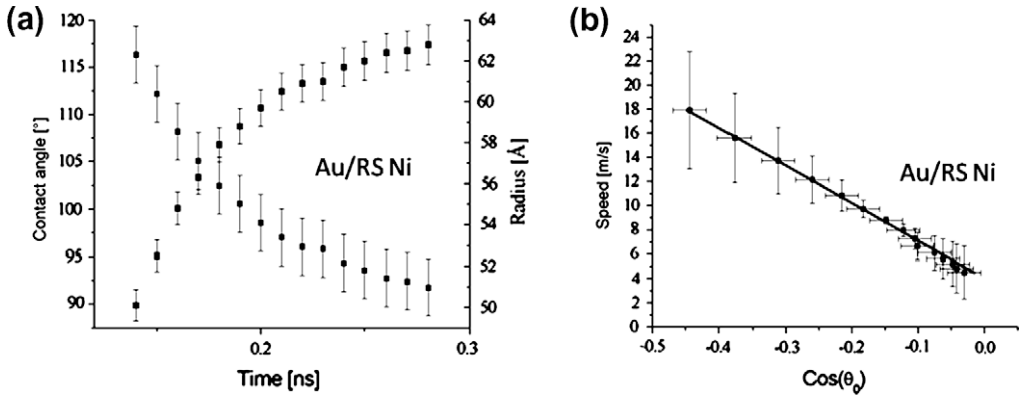

Fig. 11. Relaxation of the contact angle and growth of the base radius vs. time for Au on: (a) a regular Ni solid with (b) the corresponding wetting dynamics.

The parameters of the fits to the linear molecular kinetic model are summarized in Table 2.

3.3. Link between diffusion and friction in CS and RS

According to the MKT, what happens in the first layers of the liquid in contact with the solid surface is critical for the spreading of the liquid front, especially at the triple line [7].

Let D_s represent the diffusion in the interfacial region, D_{bulk} is the diffusion in the bulk liquid, η is the viscosity of the liquid, and ζ_0^s is the contact line friction. Bertrand demonstrated [32] that the diffusion can be related to the friction using the Stokes–Einstein formula to extract the

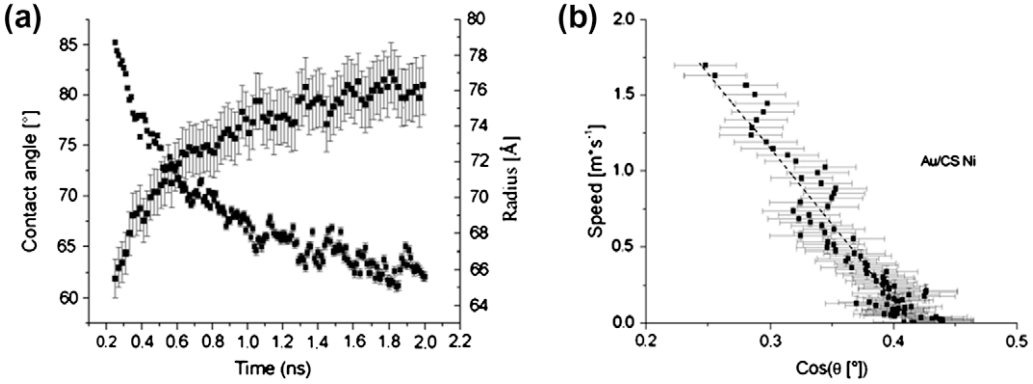

Fig. 12. (a) Gold spreading dynamics on the CS along with (b) the best fit generated by G-dyna.

Table 2
Best set of parameters for a linear MKT fitting with Ag on RS and CS as calculated by G-dyna.

	ζ_0 (Pa s) (error)	θ_0 (°) (error)
Ag 1200 K RS–Ni	0.0319 (0.0035)	85.36 (3.70)
Ag 1200 K CS–Ni	0.3457 (0.0052)	11.02 (1.23)
Au 1400 K RS–Ni	0.0398 (0.0068)	83.88 (2.85)
Au 1400 K CS–Ni	0.1708 (0.0040)	62.56 (0.16)

Table 3
Values of the diffusion and friction ratios for Ag and Au in the case of CS and RS.

	Ratio of $\sqrt{D_{x,y}}$	Ratio of ζ_0
Ag	9.955	10.837
Au	4.626	4.29

viscosity and include it in the MKT (Eq. (8) below) such that

$$\frac{D_s}{D_{bulk}} = \frac{\eta}{\zeta_0^S} \tag{6}$$

Since D_{bulk} and η are the same in the case of CS and RS (same liquid), this equation becomes

$$\frac{D_{s,RS}}{D_{s,CS}} = \frac{\zeta_0^{CS}}{\zeta_0^{RS}} \tag{7}$$

D_s is defined [32] in the layered zone (which extends 20 Å away from the solid surface according to the density profiles for Au and Ag before reaching the bulk plateau as in Fig. 4).

For Ag, the slope for CS is 9.734 (0.960) (Å $ns^{-1/2}$) and for RS 96.898 (0.803) (Å $ns^{-1/2}$). The ratio of diffusion is thus 9.955 (1.074) (results presented in Table 3), whereas the friction ratio is 10.837.

For Au, the ratio of friction is 4.29, and the diffusion ratio value is 4.626. The change in diffusion in the interfacial region seems also to explain the variation in the friction of the liquid.

The atomic displacements (diffusion, jumps over adsorption sites) and the geometry of the liquid/solid interface thus influence the macroscopic behavior (contact angle). The results are summarized in Table 3.

It is noteworthy that Eq. (6) also means that the product $D_s\zeta_0^s = \eta D_{bulk}$ remains more or less constant, because the viscosity η and the bulk diffusion for metals D_{bulk} are similar for all liquid metals (with viscosities on the order of 10^{-3} Pa s and diffusion coefficients in the range of 10^{-8}–10^{-9} m^2 s^{-1} [27]. Therefore, the friction–diffusion relation could hold for any metallic liquid.

Spreading in liquid metals involves a complex collective motion which is dependent on the formation of ordered layers in the liquid phase close to the interface [3]. Hashibon et al. [33] used exponential decay fitting (i.e., $d \sim d_0 e^{-\kappa z}$) of the liquid density to quantify the interfacial ordering.

The relaxation constant κ of the density profile can then be used to characterize the differences between CS and RS. These fits are presented in Fig. 13 (the relaxation constants are presented in Table 4). Also, the decaying length parameter $1/\kappa$ as a function of friction shows the increasing friction with increased ordering. The limiting case $\kappa = 0$ could correspond to two extreme cases: either an infinite friction (or null frequencies) consistent with ordered atoms in a solid or pure liquid with no ordering. The later would yield a finite friction that will relate to bulk liquid frequencies.

The decay length (or the inverse of the relaxation constant κ) for Ag and Au ratios are of the same order of magnitude (it increases by 60–70% from CS to RS, showing the increased ordering in CS).

In the present simulation, the first liquid layer in contact with the solid is always fully occupied. Intuitively, a lower density gradient (or a larger decay length $1/\kappa$) corresponds to a larger degree of ordering in the interface which will translate into larger occupancy (fewer vacancies) in the liquid layers close to the interface and thus reduced equilibrium frequencies K_0. This means that a stronger ordering (larger $1/\kappa$) will correspond to greater friction and slower spreading kinetics. These trends seem to be confirmed by the present results (Fig. 13).

3.4. Direct calculation of the frequencies

The atomic frequencies can be measured directly using the atomic trajectories vs. time and the method previously

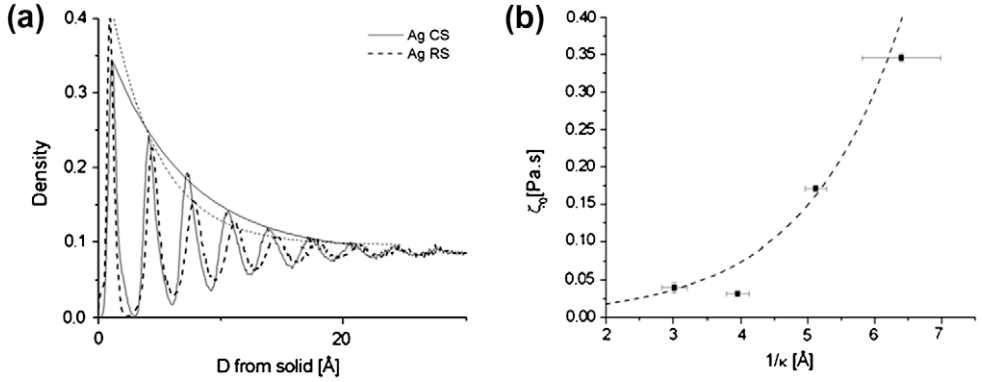

Fig. 13. (a) A decaying exponential function is used to quantify the liquid density gradients in the direction perpendicular to the interface for RS and CS substrates. (b) On the right, the inverse of the decay time (or the correlation length) $1/\kappa$ is plotted vs. the fitted friction. An increase in ordering in the commensurate case (higher correlation length) increases the friction parameter. Notice that in this interpretation, if ordering at the interface does not occur, the density of the liquid is constant ($\kappa = 0$), leading to a minimum in the friction determined by the atomic frequencies in the bulk liquid. A dashed line is added to guide the eye.

Table 4
Relaxation parameters of the decay of density across the liquid–solid interface.

$d - d_0\exp^{-\kappa Z}$	Ag RS	Ag CS	Au RS	Au CS
$1/\kappa$ (Å) (error)	3.9509 (0.1696)	6.3579 (0.5830)	3.0190 (0.1867)	5.1172 (0.1586)

described by Benhassine et al. [3]. The controlling frequencies obtained by fitting the spreading data with the linear molecular kinetic model (assuming a reasonable jump length λ of the order of interatomic distances) and those measured directly are in good agreement, supporting the validity of the theory.

4. Discussion

The agreement between fitted and measured frequencies indicates that the MKT is appropriate to describe the spreading process. Qualitatively, for Ag and Au, the behavior is the same, i.e., the growth of an adsorbed layer is slowed by the reduced surface diffusion resulting from the commensurability between Ag, Au and the solid.

Numerically, the fitted friction is 10-fold higher in CS than in the RS, corresponding to a larger liquid ordering at the interface. This increase is directly related to the diffusion in the liquid in the order region at the interface, as the ratio of the corresponding diffusion coefficients scales as the inverse of the friction coefficient.

Nevertheless, the substrate geometry (i.e., the commensurability) may not be the only factor responsible for a change in triple-line friction. The MKT theory demonstrates that a change in contact angle and spacing λ between the solid atoms can change the value of the friction [31]. Here, the final contact angles are radically different in the cases of CS and RS, and the spacing is imposed by the two different geometries from 85° to 20° for Ag with a spacing of 3–3.5 Å.

According to Blake and De Coninck [34], the friction can be related to θ_0 and λ via the relation

$$\zeta_0 = \frac{\eta_l v_l}{\lambda^3} \exp\left(\frac{\gamma_{lv}(1+\cos(\theta_0))}{n k_B T}\right) \tag{8}$$

where η_l is the liquid viscosity, v_l is the molecular volume, and n is the number of adsorption sites. k_B is Boltzmann's constant, and γ_{lv} is the liquid/vacuum surface tension. Their model relates the triple-line friction to the strength of the solid–liquid interactions (the work of adhesion) [34].

Considering a ratio of CS and RS parameters, formula (8) becomes

$$\ln\left(\frac{\zeta_0^{CS}}{\zeta_0^{RS}}\right) = \ln\left(\frac{\lambda_{RS}^3}{\lambda_{CS}^3}\right) + \frac{\gamma_{lv}}{k_B T}\left[\frac{1}{n_{CS}}(1+\cos(\theta_0^{CS})) - \frac{1}{n_{RS}}(1+\cos(\theta_0^{RS}))\right] \tag{9}$$

The fitted parameters imply that the left member of Eq. (9) is 2.383 for Ag and 1.457 for Au, but the right member is evaluated as 4.739 for Ag and 4.531 for Au. In order to show that these values are different, one must estimate the errors associated with the parameters to demonstrate whether there is an overlap of the calculated values.

A population is generated by taking into account the errors on the fitted parameters (generating points out of a normal distribution with the mean as the peak and the error as one standard deviation). The two members of Eq. (9) are evaluated independently in Fig. 14. There is no overlap between the curves, demonstrating that, even taking the errors into account, Eq. (8) is not able to explain the variation in friction between the two substrate geometries. It demonstrates that the atomic arrangement of a liquid/solid interface has an important role in the equilib-

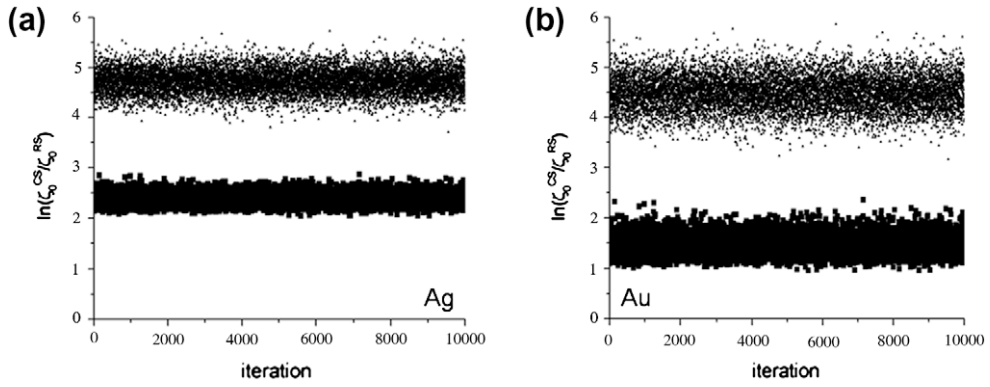

Fig. 14. The two members of Eq. (9) are evaluated independently (the left member is represented by squares and the right member by triangles) from the generated populations of the parameters (λ^{CS}, λ^{RS}, θ_0^{CS} and θ_0^{RS}). (a) Ag is presented on the left, and (b) Au is displayed on the right.

rium values of the contact angle and the friction of liquid metals. What is remarkable is that the increase in friction parameter by an order of magnitude between commensurate and non-commensurate substrates cannot be explained by the possible small differences in λ and, rather, seems related to the increase in interfacial ordering resulting from matching solid and liquid structures.

Theoretically, Eq. (8) is based on the assumption that the wetting activation energy is related to the work of adhesion. Although well validated for organic liquids, it was demonstrated experimentally [2] that this relation might not be valid for liquid metals where spreading is controlled by a complex collective motion in which the role of interfacial ordering seems to be determinant. This is also consistent with weaker solid–liquid interactions in organic liquids which will result in much decreased ordering and a situation closer to one of the $\kappa = 0$ limits. Nonetheless, the agreement of Eq. (6) with the present data suggests that the friction–diffusion relation still remains valid.

5. Concluding remarks

The effect of the lattice mismatch on the spreading of liquid metal (Ag, Au) drops on rigid solid Ni substrates was studied by means of molecular modeling. The presence of the solid substrate induced some degree of ordering in the liquid near the interface and the formation of a layered region. This ordering extends to distances up to ~20 Å away from the first layer of solid atoms and results in a density gradient. The spreading kinetics can be described using the MKT theory, and the corresponding triple-line frictions can be calculated. The results are similar for silver or gold. A monolayer of adsorbed atoms was observed on the surface of RS ahead of the liquid front. This layer did not form on the commensurate surfaces where the lattice parameter is adjusted to fit the equilibrium value for Au or Ag and the liquid atoms were trapped by the fixed solid Ni atoms. Substrate commensurability increases ordering, decreasing the number of vacancies near the interface and reducing atom mobility. As a consequence, the in-plane diffusion kinetics in the layered region is significantly lowered and the triple-line friction is augmented in the same proportion. The degree of liquid ordering near the interface can be quantified using a characteristic decaying length $1/\kappa$ for the density gradient. This parameter can be directly related to the friction, providing further proof that atomic ordering at the solid–liquid interface in liquid metals controls transport phenomena such as spreading or diffusion.

Acknowledgements

M. Benhassine acknowledges funding from the FNRS of Belgium under the Fonds pour la Formation à la Recherche dans l'Industrie et dans l'Agriculture. This work was also supported by the Director, Office of Science, Office of Basic Energy Sciences, Division of Materials Sciences and Engineering, of the US Department of Energy under Contract No. DE-AC02-05CH11231.

Appendix A. Supplementary material

Supplementary data associated with this article can be found, in the online version, at doi:10.1016/j.actamat.2009.11.049.

References

[1] Saiz E, Tomsia AP. Nat Mater 2004;3:903–9.
[2] Saiz E, Tomsia AP, Rauch N, Scheu C, Rühle M, Benhassine M, Seveno D, De Coninck J, Lopez-Esteban S. Phys Rev E 2007;76:041602.
[3] Benhassine M, De Coninck J, Saiz E, Tomsia AP. Langmuir 2009;25(19):11450–8.
[4] Webb III EB, Hoyt JJ, Grest GS. Curr Opin Solid State Mater Sci 2005;9:174–80.
[5] Webb III EB, Grest GS, Heine DR. Phys Rev Lett 2003;91(23):236102.
[6] Deltour P, Barrat JL, Jensen P. Phys Rev Lett 1997;78(24):4597–600.
[7] Blake TD. In: Berg JC, editor. Wettability. New York: Marcel Dekker; 1993. p. 251–309.
[8] Petrov JG, Ralston J, Schneemilch M, Hayes R. J Phys Chem B 2003;107:1634.
[9] Blake TD. J Colloid Interf Sci 2006;299:1.
[10] Ralston J, Popescu M, Sedev R. Ann Rev Mater Res 2008;38:23.

[11] de Ruijter MJ, Blake TD, De Coninck J. Langmuir 1999;15:7836.
[12] Blake TD, Haynes JM. J Colloid Interf Sci 1969;29:174.
[13] Blake TD. PhD thesis, University of Bristol; 1968.
[14] Plimpton SJ. J Comp Phys 1995;117:1–19.
[15] Stevens M, Plimpton SJ, Pollock R. In: Proc eighth SIAM conference on parallel processing for scientific computing, Minneapolis (MN); 1997.
[16] Daw MS, Baskes MI. Phys Rev B 1984;29:12:6443–6453.
[17] Foiles SM, Baskes MI, Daw MS. Phys Rev B 1986;33:7983–91.
[18] Hashibon A, Adler J, Finnis M, Kaplan WD. Comput Mater Sci 2002;24(94):333.
[21] Hashibon A, Lozovoi AY, Mishin Y, Elsässer C, Gumbsch P. Phys Rev B 2008;77:094131.
[22] Bertrand E, Blake TD, Ledauphin V, Ogonowski G, De Coninck J, Fornasiero D, et al. Langmuir 2007;23:3774.
[23] Blake TD, Clarke A, De Coninck J, de Ruijter MJ. Langmuir 1997;13:2164.
[24] Seveno D, Vaillant A, Rioboo R, Adao H, Conti J, De Coninck J. Langmuir 2009;25(22):13034–44.
[25] Moon J, Yoon J, Wynblatt P, Garoff S, Sutter RM. Comput Mater Sci 2002;25:503–9.
[27] Gale WF, Smithells CJ, Totemeier TC, editors. Smithells metals reference book. Oxford: Elsevier; 2004.
[28] Akhter JI, Ahmed E, Ahmad M. Mater Chem Phys 2005;93(2–3):504–7.
[29] Valignat MP, Bardon S, Villette S, Cazabat AM. Fluid Phase Equilibr 1998;150–151:615–23.
[30] Brochard-Wyart F, di Meglio JM, Quéré D, de Gennes PG. Langmuir 1991;7:335.
[31] Wynblatt P, Humfeld KD, Garoff S. Langmuir 2004;20:2726–9.
[32] Bertrand E, Blake TD, De Coninck J. Molecular kinetic theory of dynamic wetting: application to slip, in preparation.
[33] Hashibon A, Adler J, Finnis MW, Kaplan WD. Interf Sci 2001;9:175–81.
[34] Blake TD, De Coninck J. Adv Colloid Surf Sci 2002;96:21–36.